

Visualization of Unsteady Fluid Flows by Using Large Eddy Simulation

Toshio Kobayashi*, Nobuyuki Taniguchi

Institute of Industrial Science, University of Tokyo, 4-6-1 Komaba, Tokyo, Japan

Three-dimensional and unsteady flow analysis is a practical target of high performance computation. As recently advances of computers, a numerical prediction by the large eddy simulation (LES) are introduced and evaluated for various engineering problems. Its advanced methods for the complex turbulent flows are discussed by several examples applied for aerodynamic designs, analysis of fluid flow mechanisms and their interaction to complex phenomena. These results of time-dependent and three-dimensional phenomena are visualized by interactive graphics and animations.

Key Words : Numerical Simulation, Turbulent Flow, Large Eddy Simulation

1. Introduction

A recent recognition in an environmental situation and a limitation of energy resource requires us to innovate new technology more adaptive engineering to strict requirements and worldwide standards. For this aim, design optimization has been investigated in their various and complex conditions, where a key technology should be developed on fundamental studies of three-dimensional and unsteady features in fluid flows. While recent innovations of computers give us a remarkable advance in the computer-aided engineering (CAE) in the fluid dynamics researches, which enables numerical simulation and visualization applied to the three-dimensional and unsteady analysis of turbulence in detail and directly.

A numerical simulation has been successfully applied to various turbulence phenomena (Kobayashi and Taniguchi, 1997). A practical approach based on the statistical turbulence model has difficulty to apply for the complex and unsteady interaction of turbulence, while a direct

numerical simulation (DNS) is limited only in microscopic phenomena though it has revealed fundamental processes of the turbulent flows (Tanahashi, et al., 1997). A large eddy simulation (LES) is alternative possible approach within the limited computer resource, which can directly analyze an unsteady and complex interaction of turbulence using a theoretical modeling and a practical numerical method. The LES has been investigated in the various applications, not only fundamental flows but more complex object such as turbulent mixing processes in an impinging jet (Tsubokura, et al., 1997), oscillating wake behind a cylinder (Kogaki, 1999) etc. In these researches, turbulence models and numerical methods are developed for treating three-dimensional and unsteady characteristics of turbulence directly, and their accuracy and reliability are also discussed.

This paper introduces the above applications for the three-dimensional and unsteady analysis of turbulent flows and evaluates their feasibility for the engineering design, for examples, a prediction and a control of fluid flows.

2. Methods of Analysis

2.1 Basic equations of LES

The LES calculates the grid scale (GS) fluid

* Corresponding Author,

E-mail : kobaya@iis.u-tokyo.ac.jp

TEL : +81-3-5452-6196; FAX : +81-3-5452-6197

Institute of Industrial Science, University of Tokyo, 4-6-1-Komaba, Tokyo, Japan. (Manuscript Received September 25, 2001; Revised October 10, 2001)

motions that can be resolved by the computation grid directly, while it models only the subgrid scale (SGS) fluctuations that are smaller than the grid resolution. For the incompressible flows, the governing equations of the GS component are described as follows,

$$\frac{\partial \bar{u}_i}{\partial x_i} = 0 \quad (1)$$

$$\frac{\partial \bar{u}_i}{\partial t} + \frac{\partial \bar{u}_i \bar{u}_j}{\partial x_j} = -\frac{\partial \bar{p}}{\partial x_i} + \nu \frac{\partial^2 \bar{u}_i}{\partial x_j^2} + \frac{\partial \tau_{ij}}{\partial x_j} \quad (2)$$

where the variables \bar{u}_i , \bar{p} denote the filtered velocity and pressure in the grid resolution space. The last term, τ_{ij} in the momentum equation (Eq. 2) represents the SGS stress and is approximated by a Smagorinsky model (Smagorinsky (1963), see also Deardroff (1970)) as follows,

$$\tau_{ij} \equiv \overline{u_i u_j} - \bar{u}_i \bar{u}_j = \nu_{SGS} \bar{S}_{ij}, \quad \nu_{SGS} = (C_S \Delta)^2 |\bar{S}| \quad (3)$$

Here, \bar{S}_{ij} and $|\bar{S}|$ are a strain rate tensor and its norm, and Δ denotes a filter width. A model parameter C_S called a Smagorinsky constant should be optimized to the types of flows; for examples, $C_S=0.1$ for the developed flows in the parallel channel or the circular pipe and 0.12~0.15 for the wake or the jet flows are mostly adopted in the previous researches, otherwise for the homogeneous turbulence in the weak shear 0.17~0.2 is theoretically evaluated. Then Germano et. al. (1991) proposed a new concept of SGS model, called a "dynamic" model, which formulates the optimized value of C_S by using the information of the numerical solution simultaneously (see also Lilly (1992), Meneveau et. al. (1994)). This approach gives an universal optimization scheme, which seems such an appropriate improvement as to apply the LES to the unknown types of flows and also to extend it to the newly developed models for the complex flows.

However, it should be noted that the choice of the SGS models is not a primal problem in the most practical LES applications because the GS solution usually more contributes to the calculation results. Compared to another approach based on the Reynolds average models, it is a remarkable merit of LES that finer grid generally makes more accurate result. Any LES should converge

to DNS when using a grid fine enough to resolve the minimum scale of turbulence fluctuation. Then an effect of the SGS model varnishes.

2.2 Modeling of reaction flows

For turbulence combustion flows, chemical reaction usually proceeds much faster than the typical frequency of turbulence fluctuation, so as that the equation system including the both features becomes too stiff to solve directly. In LES it is a reasonable approximation that only the flame propagation deformed by turbulent large eddies is solved in the GS field and the local interaction to the chemical reaction is model as a SGS effect. For examples, the premixed flame propagation is expressed by Williams (1985) and its LES formulation was derived by Kerstein et. al. (1988), as follows,

$$\frac{\partial \bar{G}}{\partial t} + \frac{\partial \bar{u}_j \bar{G}}{\partial x_j} = \frac{\partial \gamma_i}{\partial x_j} + S_L |\nabla \bar{G}|, \quad \gamma_i = \bar{u}_i \bar{G} - \overline{u_i G} \quad (4)$$

Here, S_L is a propagation speed in laminar flame then the preset isosurface of scalar property $G=G_0$ represents the premixed flame front. According to the flamelet concept, it is assumed that each local element of flame propagates in the same manner as the laminar flame. However, in LES the smaller flame deformations than the resolved velocity field can not be captured, the effects of which are expressed in the two terms of the right hand side; the former is modeled as a SGS diffusion and the later is re-written as,

$$S_L |\nabla \bar{G}| = S_{GS} |\nabla \bar{G}| \quad (5)$$

Eq. (5) means that by the effects of the unsolved SGS fluctuation, the flame in the GS field seems thicker and to propagate faster than the laminar flame (e. g. $S_L < S_{GS}$). According to the empirical studies, for examples, it is modeled by

$$\frac{S_L}{S_{GS}} = 1 + C_\alpha \left(\frac{q}{S_{GS}} \right)^n, \quad n=1 \sim 2 \quad (6)$$

Here, in LES, the turbulence velocity scale u' can be related to the SGS kinetic energy. Coefficients in the above turbulent models are optimized by fundamental studies, otherwise the dynamic model is also applicable (Im et. al. (1997), Park et. al. (2000)).

Table 1 Specifications of model engine

| | |
|----------------------|----------------------|
| Combustion chamber | pancake-shaped |
| Number of valve | one intake / exhaust |
| displace volume | 411 (cc) |
| Bore* stroke | 82*78 (mm) |
| Compression. ratio | 13.5 |
| top clearance | 1.0 (mm) |
| intake valve open | 15°C BTDC |
| intake valve close | 15°C ABDC |
| exhaust valve open | 15°C BBDC |
| exhaust valve close | 15°C ATDC |
| Valve diameter in/ex | 32/28 (mm) |
| Max. valve lift | 8 (mm) |
| engine speed | 240 (rpm) |

3. Calculation Results and Their Visualizations

3.1 Applications to engineering design

Analysis of complex flows under unsteady conditions may become attractive objects of high-performance computing. It has been investigated in various engineering fields with requirement of more practical predictions and designs. At the first example, a flow in the intake and compression strokes of a four-cycle gasoline engine was analyzed by Zhang & Kobayashi (2000). The specification of model engine conditions and computation domain are indicated in Table 1 and Fig. 1, respectively. The grid system is generated by ICEM pre-process code. Multi-block method is used in order to keep the orthogonality of grid arrangement. The entire calculation domain is divided into six blocks and the number of total nodes was about 640,000. The information interchange between the every two blocks is carried out on "iteration-by-iteration" level and "time-step by time-step" level. The overlap grids on every interface boundary are regarded as virtual grids for each other. For analyzing the piston and valve motions, the re-meshing in their parts were introduced in each time step, too.

In Fig. 4 time-marching flow patterns are

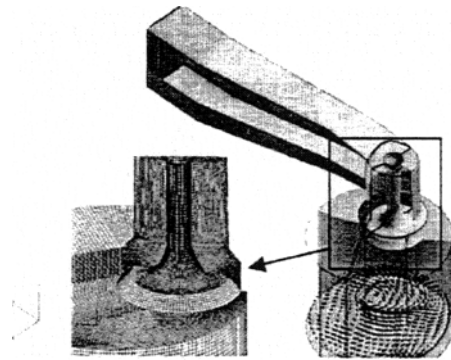


Fig. 1 whole computational domain and grid arrangement in detail

visualized by streamlines to understand flow image in cylinder flow, which can be divided into three stages. The first stage (0°C to 75°C) is in piston acceleration process, when the swirl velocity is very weak (remarkable swirl center is not formed in Fig. 2) and the axial velocity is strong due to the acceleration of piston. The turbulence intensity is intensive generated by the intake-valve and the moving piston, too. The second stage (75°C to 180°C) is in piston deceleration process. In this stage, downward moving discharge is decelerated by piston. Swirl velocity is gradually formed and is strengthened with piston deceleration. The deceleration of piston transfers the downward movement into the swirl moment. At 120°C, the swirl gets its peak value, but in this stage the turbulence intensity becomes weaker gradually. At the 180°C velocity vectors in the middle horizontal section and their centerline profile are compared with experimental data by particle image velocimetry (PIV) to the motored engine model (Figs. 3, 4). They probed this simulation predict the swirl generation in the cylinder correctly. The third stage (180°C to 360°C) is in compression process. In this stage, the piston is in the condition of up-ward movement and the outside disturbance disappears in cylinder. The swirl flow is confined by cylinder shape and its center tends to move to the cylinder centerline. A swirl number is not weakened obviously by wall friction of cylinder. Because of no outside disturbing, turbu-

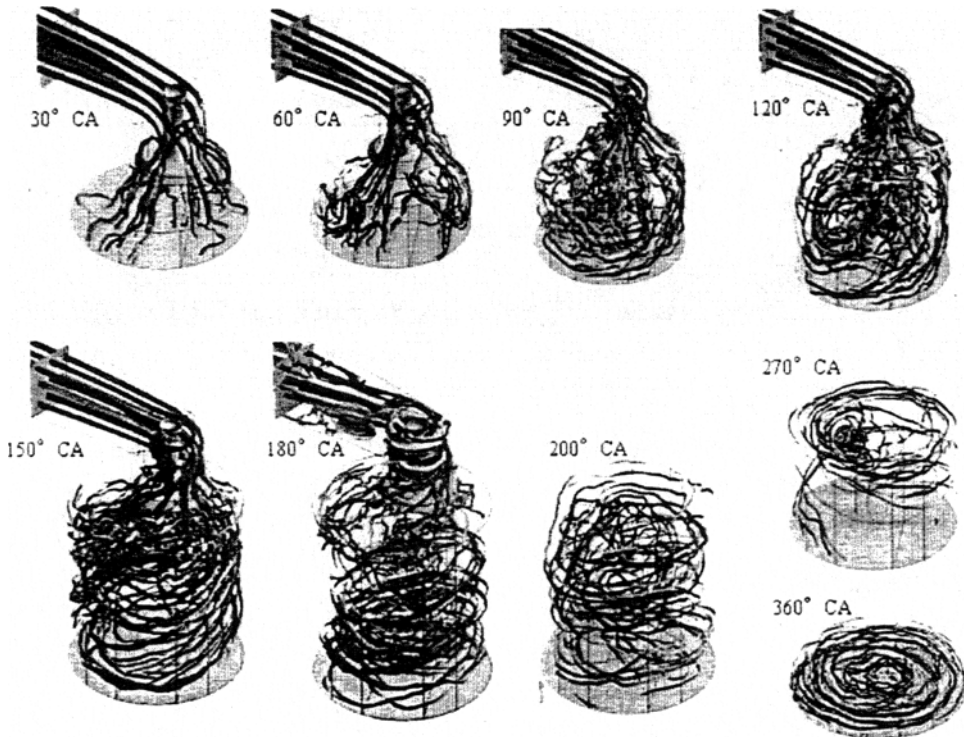


Fig. 2 Instantaneous streamline at nine crank angle positions

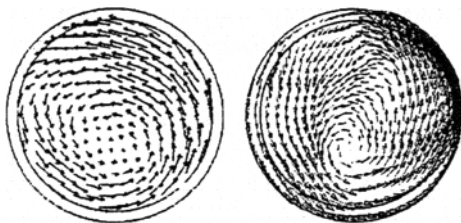


Fig. 3 Velocity vector of PIV (left) and LES (right) at 180°CA

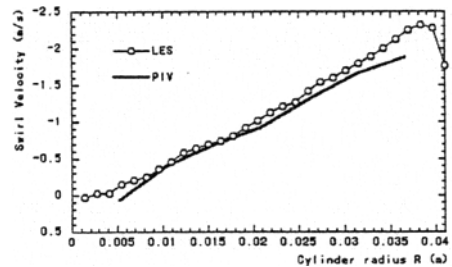


Fig. 4 Comparison of mean Swirl velocity between the PIV experiment and LES calculation at 180°CA

lence intensity is gradually weakened.

Another application was conducted by Kato (1995; 2000) for analyzing aerodynamic noise from the pantograph of the high-speed train. In this case for treating a more complicated shape, a finite element method (FEM) with around 6 million nodes was adopted for capturing the reality of their complicated shape effects. Figure 5 shows a three-dimensional profile of the reverse flow region and a sound source distribution in the

rear section at the same instantaneous time. These visualization indicated that the sound sources appeared in the strong shear layer of rear wake and also that the streamwise vortices generated by the layered structures corresponded to the high-frequency noises. Shown in this case, the observation from LES results can reveal an unsteady mechanism of noise generation and contributes to the noise reduction, though the LES for the external flows tends to take more cost than the

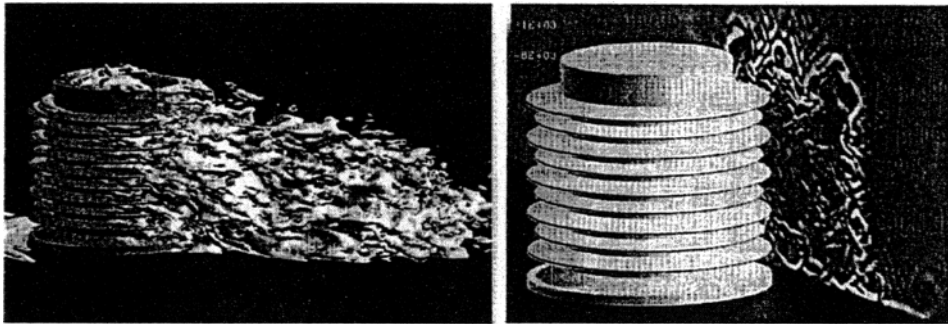


Fig. 5 Visualization of LES result for flow around a part of pantograph of high-speed train (left: instantaneous reverse flow region, right: instantaneous sound source distribution)

internal flows as the previous one. Similar simulations are also applied for the aerodynamic designs of aircrafts and automobiles.

3.2 Predictions of combustion flows

As an example of power generation engineering, the analysis techniques mentioned above were applied to the flow design of the gas-turbine combustor (Taniguchi et al., 1999; Itoh, 2000). An aim of this research was to develop a numerical prediction of turbulent combustion flows with the LES for a systematical design of the clean and high-efficient combustion equipment. A numerical method and a model mentioned above were validated for the premixed combustion flows in a test combustion section of the gas-turbine system. The computational domain was defined as an experiment test section for the gas turbine combustor shown in Fig. 6. Typical situations of the target experiment are listed in Table 2. A premixed gas discharged into a sudden expansion impinges on the circular flame holder and generates a separated region holding the flame behind the holder. A fuel pipe (0.1D) supporting the flame holder from the inlet position is neglected in the present calculation. Turbulent flows of Reynolds number 50, 000 (match to experiment) based on the inlet mean velocity (U_{in}) and the diameter (D) of the flame holder are performed by the LES. A number of grid points are $55 \times 90 \times 102$ (504, 900) in the radius (r), circumference (θ) and streamwise directions (z), respectively, so that a typical grid size is $0.01D$ near the flame holder. A non-

Table 2 Experimental conditions of test chamber

| | Non-flame | Flame |
|-------------------|-------------------------|-------------------------|
| Inlet velocity | 28.4 m/s | 24m/s |
| Cooling air velo. | 0.0 m/s | 5~20 m/s |
| Air rate | 121 Nm ² /h | 70 Nm ² /h |
| Fuel rate | - | 3.8 Nm ² /h |
| Fuel ratio | - | 0.03 |
| Flame temp. | - | 1370°C |
| Inlet air temp. | 17 °C | 120°C |
| Press. cham. | 1.0 kgf/cm ² | 1.0 kgf/cm ² |

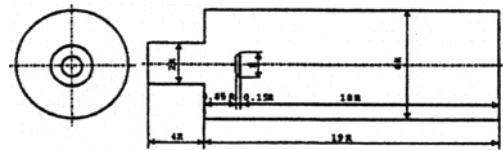


Fig. 6 Configuration of combustion test chamber

dimensional time increment is $\delta T = 0.002$ and the calculation is carried out from a laminar solution imposed a random fluctuation till the turbulent statistical values are developed so that they are evaluated after $T > 40$. The calculation is performed on a Silicon Graphics-Origin2000 and a Fujitsu-VX. A typical CPU time is about 5 min/step or 0.8 min/step on these computers, respectively.

Figure 7 shows the G -profiles in the developing stages predicted by LES, which illustrate the flame propagation of flame predicted. An animation is more available to understand a flame propagation process practically (Itoh et al., 2000). Following to the LES result, in the early stage the flame behind holder was intermittently transferred to downstream by the fluctuating

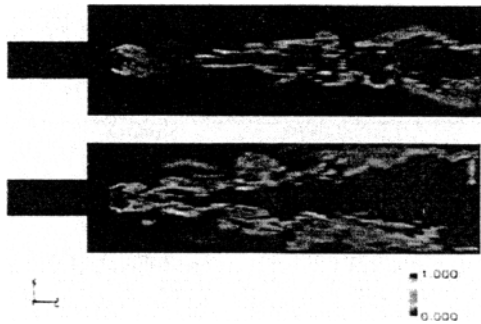


Fig. 7 LES prediction of flame propagation in combustion chamber; G-profiles at $T = 42$ (~ 10 ms latter after lighten) (above), and at $T = 44$ (~ 20 ms) (below)



Fig. 8 Three-dimensional view of the developed flame ($T = 50$) by the iso-surface level $G = 0.5$

wake, and propagated along the center line to both way (Fig. 7 above), then develop to the wall to fill the whole chamber (Fig. 7 below). Figure 8 shows a instantaneous three-dimensional profile of the developed flame by the iso-surface level of scalar G , when the burned level was 'held' in the separation behind the flame holder and filled in the whole section downstream at $z \sim 3D$.

4. Conclusion Remarks

Turbulent flows contain highly three-dimensional and unsteady vortical structures which interact each other and also influence in transport phenomena. Numerical simulations by the LES are available to analyze the multi-scale and/or intermittent phenomena in turbulence which are difficult to captured in the averaged data by the traditional methods. For this purpose they generally need high resolution in space and

time, which has been developed by recent investigators. The precise unsteady analyses indicate the mechanism of complex turbulent transport directly, while it also revealed some defects and limitation in the flow predictions.

References

- Deardorff, J. W., 1970, "A Numerical Study of Three-Dimensional Turbulent Channel Flow," *J. Fluid Mech.* 118, pp. 341~377.
- Germano, M., Piomelli, U., Moin, P., Cabot, W. H., 1991, "A Dynamic Subgrid-Scale Eddy Viscosity Model," *Phys. Fluids A3*, pp. 1760~1765.
- Im, H. G., Lund, T., Ferziger, J. H., 1997, "Large Eddy Simulation of Turbulent Front Propagation with Dynamic Subgrid Models," *Phys. Fluids* 9 (12), pp. 3826~3833.
- Itoh, Y., Taniguchi, N., Masaki, K., Kobayashi, T., 2000, "Large Eddy Simulation of a Premixed Combustion Flow in a Gas Turbine Combustor," ISFV-6.
- Kato, C. et al., 1995, "Numerical Simulation of Aerodynamic Sound Radiation from Low Mach Number Turbulent Wakes," *ASME FED* 219, pp. 53~58.
- Kato, C., 2000, "Present Status and Future Promise of Computational Aeroacoustics," *Monthly J. of Institute of Industrial Science (SEISAN-KENKYU)*, University of Tokyo 52 -1, pp. 3~8.
- Kerstein, A. R., Ashurst, W. T., Williams, F. A., 1988, "Field Equation for Interface Propagation in an Unsteady Homogeneous Flow Field," *Physical Rev.* A37-7, pp. 2728~2731.
- Kobayashi, T. and Taniguchi, N., 1997, "Feasibility of the LES for Engineering Problems," *Int. J. Numerical Methods for Heat & Fluid Flow* 7-2/3, pp. 236~249.
- Kogaki, T., 1999, "Finite Different Schemes in Generalized Coordinates and Their Application to Large Eddy Simulation," Thesis of University of Tokyo, Dept. of Mechanical Eng.
- Lilly, D. K., 1992, "A Proposal Modification of the Germano Subgrid-Scale Closure Method," *Phys. Fluids A4*, pp. 633~635.

- Manevau, C. Lund, T. S. Cabot, W., 1994, "A Lagrangian Dynamic Subgrid-Scale Model for Turbulence," *Proc. of Summer Seminar Program, Center for Turbulence Research NASA/Stanford Univ.* pp. 1~29.
- Park, N., Kobayashi, T., Taniguchi, N., 2000, "Application of Flame-Wrinkling LES Combustion Models to a Turbulent Premixed Combustion around Bluff Body," *Int. Symposium on Turbulence, Heat & Mass Transfer*, Nagoya.
- Smagorinsky, J., 1963, "General Circulation Experiments with the Primitive Equations - I. The Basic Experiment," *Mon. Weather Rev.* 91, pp. 99~164.
- Tanahashi, M. Miyauchi, T. Ikeda, J., 1997, "Scaling law of coherent fine scale structure in homogeneous isotropic turbulence," *Proc. of 11th Symposium on Turbulent Shear Flow*, 4. 17~22.
- Taniguchi, N., Kobayashi, T., Ko, S., Ikegawa, M., 1999, "Large Eddy Simulation of a Premixed Combustion Flow in a Gas Turbine Combustor," *Proc. of Int. Joint Power Generation Conference, ASME-FACT-23*, pp. 245~254.
- Tsubokura, M. Kobayashi, T. Taniguchi, N., "Large Eddy Simulation of Plane Impinging Jets," *Proc. of 11th Symposium on Turbulent Shear Flow*, 22. pp. 24~29.
- Williams, F. A., 1985, *Turbulent Combustion, Mathematics of Combustion* (ed. J. Buckmaster), SIAM, Philadelphia.
- Zhang, H., Kobayashi, T., Taniguchi, N., 2000, "Large Eddy Simulation of Mortored Engine," *FISITA Automotive Congress F2000A008*, Seoul.